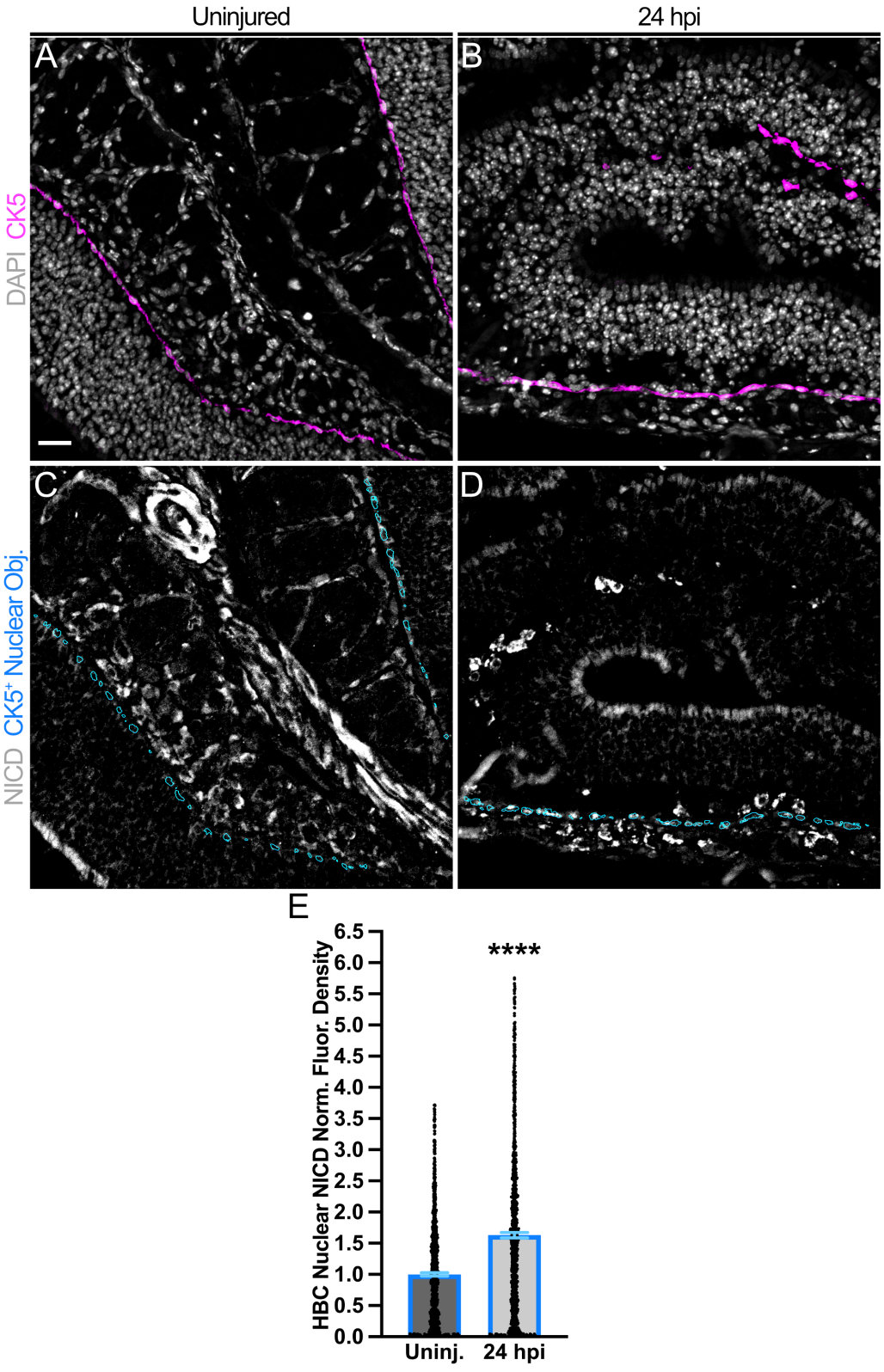

Fig. S1. HBCs at 24 hpi demonstrate increased Notch signaling pathway activity. A-D: Relative to their counterparts within uninj. OE (A), HBCs at 24 hpi (B) increase Notch signaling pathway activity given their increase in nuclear NICD. Expression of NICD within HBC nuclei demarcated in blue (C, D) is that of $CK5^+$ HBCs illustrated in their respective conditions (A, B). E: Quantification of HBC nuclear NICD norm. fluor. density, each point represents a $CK5^+$ Nuclear Object (Obj.) (as represented by blue outlines in C and D) (n = 3 mice; 1,159 Uninj. HBCs and 1,037 24 hpi HBCs). Uninj. used as baseline, error bars indicate mean ± s.e.m., Mann-Whitney test, ****$p<0.0001$ (E). Scale bar equals 25 μm (A).

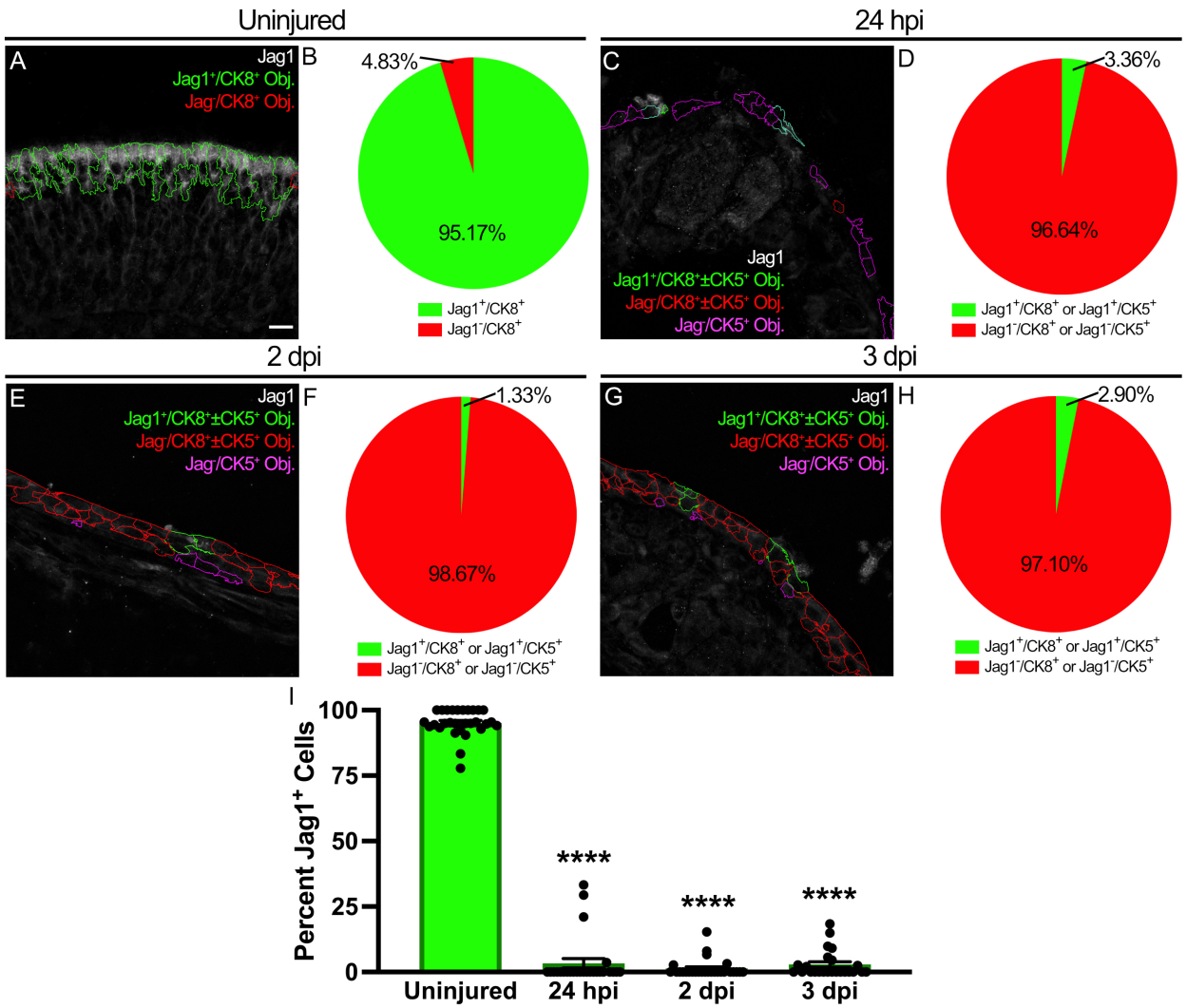

Fig. S2. Jagged1 expression is negligible during early OE regeneration. A, B: Jagged1 is highly expressed within the uninjured OE and localizes to CK8$^+$ Sus cells. C-H: As regeneration proceeds from 24 hpi (C, D), 2 dpi (E, F), and 3 dpi (G, H), scant CK5$^+$ and CK8$^+$ cells that compose the regenerating OE are Jagged1$^+$. I: Each point represents an analyzed region as represented in A, C, E, and G (n = 3 mice, 517 Uninjured CK8$^+$ cells across 29 regions, 583 24 hpi CK8$^+$ or CK5$^+$ cells across 26 regions, 988 2 dpi CK8$^+$ or CK5$^+$ cells across 27 regions, and 1,102 3 dpi CK8$^+$ or CK5$^+$ cells across 24 regions), error bars indicate mean ± s.e.m., Kruskal-Wallis test with post-hoc Dunn's multiple comparisons test, ****p<0.0001. Scale bar equals 10 μm (A).

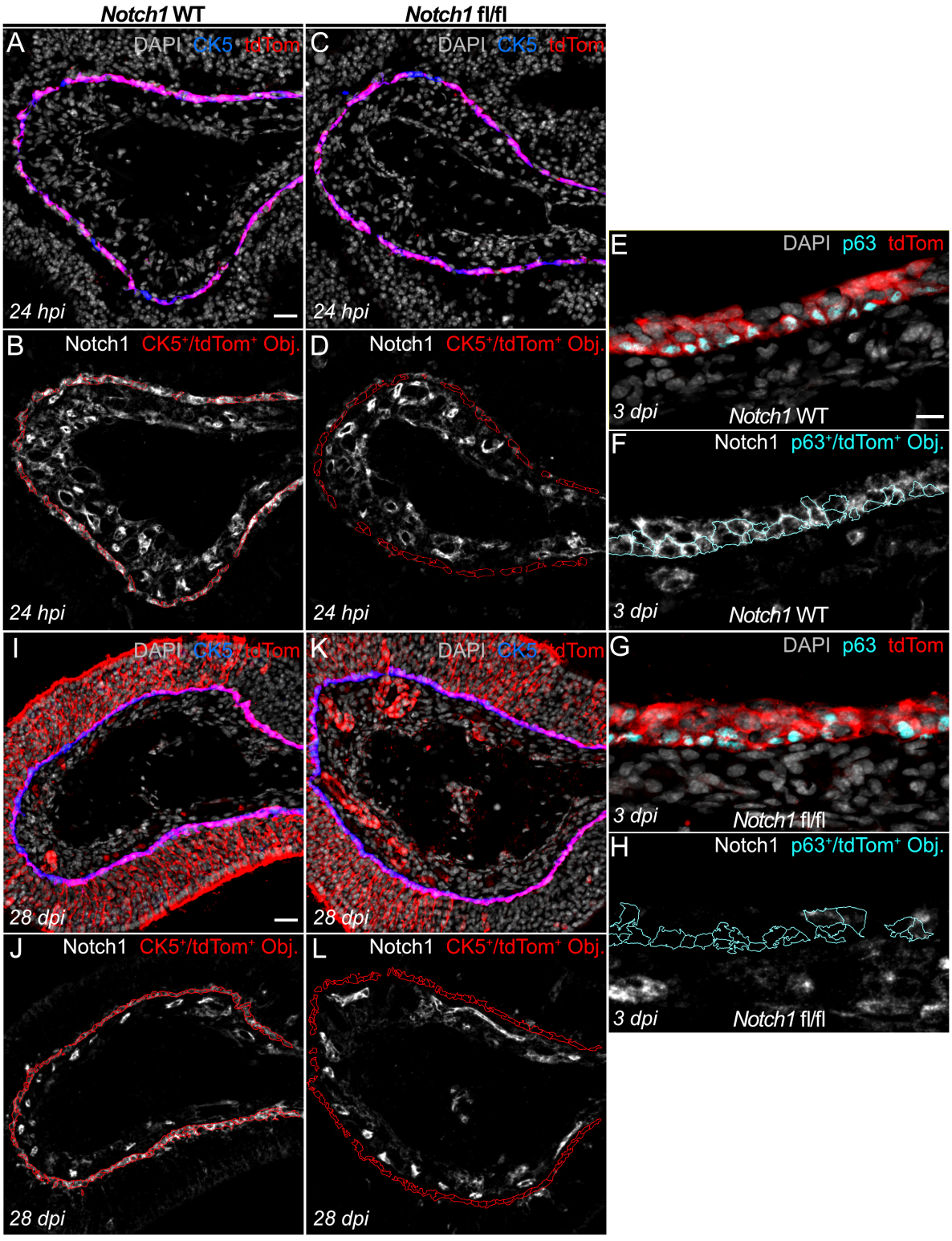

Fig. S3. *Notch1* cKO at various stages of OE regeneration. Images representing the effect of tamoxifen-induced recombination on Notch1 expression within tdTom$^+$ HBCs (red outlines, B, D, J, and L; cyan outlines, F and H) at 24 hpi (A-D), 3 dpi (E-H), and 28 dpi (I-L). Scale bars equal 25 μm (A, I) and 10 μm (E).

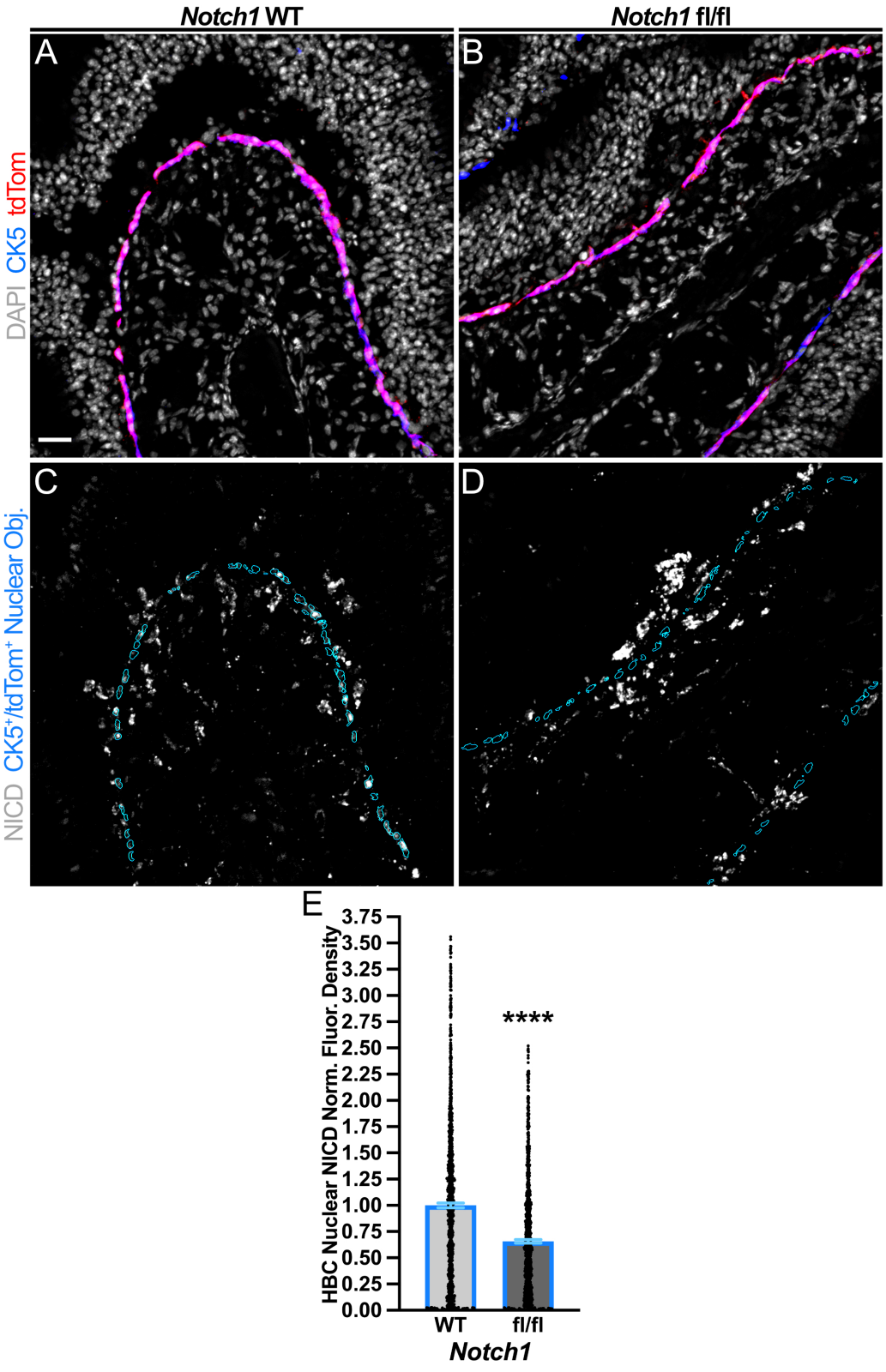

Fig. S4. Notch signaling pathway activity at 24 hpi is attenuated by HBC-specific *Notch1* cKO. A-D: Relative to those within *Notch1* WT OE (A), HBCs at 24 hpi within *Notch1* fl/fl OE (B) demonstrate diminished Notch signaling activity as evidenced by decreased nuclear NICD (within blue outlines, C and D). E: Quantification of HBC nuclear NICD norm. fluor. density, each point represents a $tdTom^+$ Nuclear Obj. (as represented by blue outlines in C and D) (n = 3 mice, 1,280 *Notch1* WT HBCs and 1,157 *Notch1* fl/fl HBCs). Error bars indicate mean ± s.e.m., Mann-Whitney test, ****p<0.0001 (E). Scale bar equals 25 μm (A).

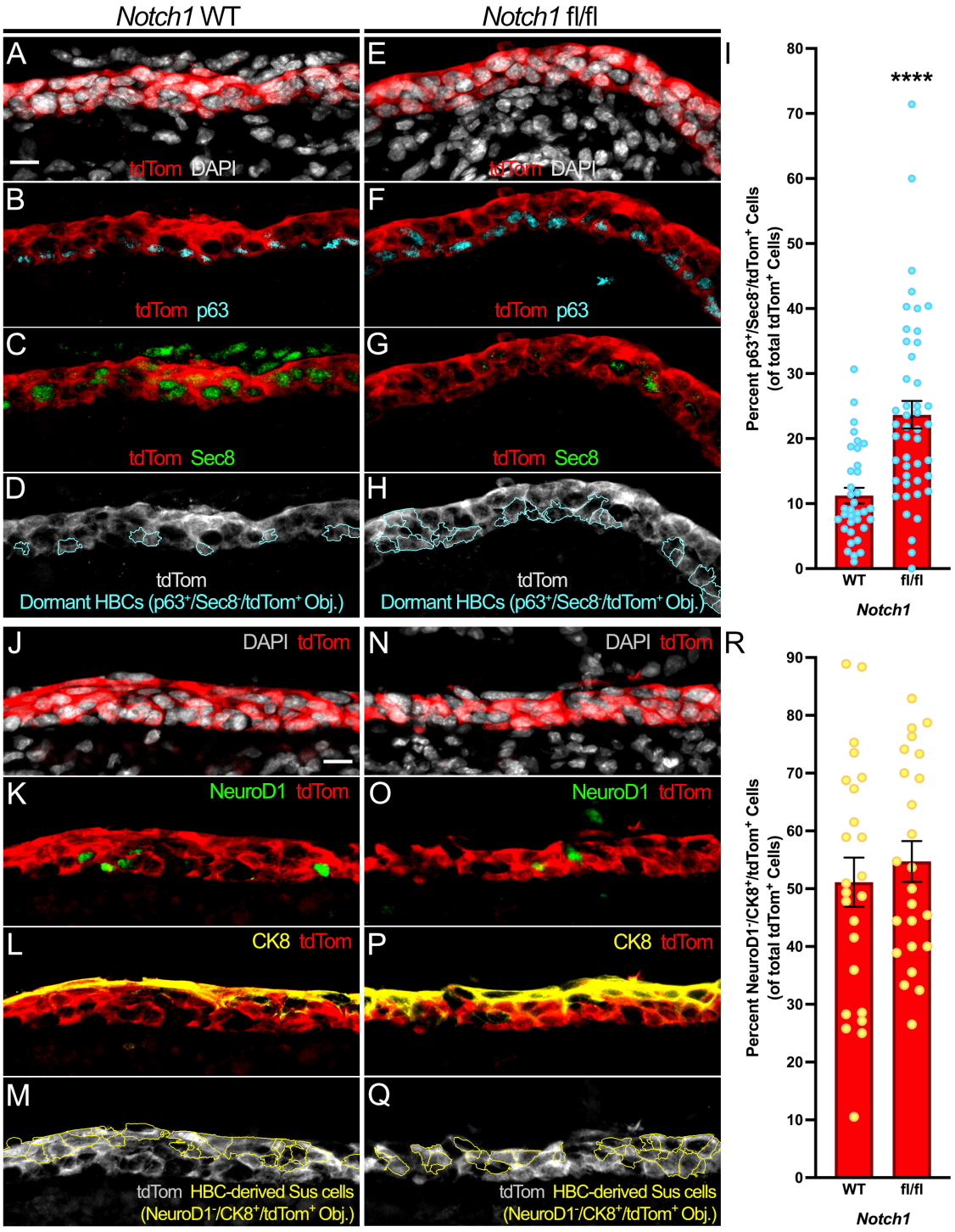

Fig. S5. *Notch1* cKO increases proportion of dormant HBCs but does not affect Sus cell composition of the regenerating OE at 3 dpi. A-H: Relative to control (A-D), the proportion of dormant HBCs (cyan outlines, D and H) amongst all HBC-derived cells within the regenerating OE at 3 dpi decreases following HBC-specific *Notch1* cKO (E-H). I: Each circle represents an analyzed region as represented in D and H (n=3 mice, 35 *Notch1* WT regions and 46 *Notch1* fl/fl regions). J-Q: Relative to control (J-M), the proportion of HBCs that differentiate into NeuroD1$^-$/CK8$^+$/tdTom$^+$ Sus cells (yellow

outlines, M and Q) within the regenerating OE at 3 dpi does not significantly change following HBC-specific *Notch1* cKO (N-Q). R: Each circle represents an analyzed region as represented in M and Q (n = 3 mice, 24 *Notch1* WT regions and 24 *Notch1* fl/fl regions). Mann-Whitney test (I), unpaired t-test (R). Error bars indicate mean ± s.e.m., ****p<0.0001 (I, R). Scale bar equals 10 μm (A).

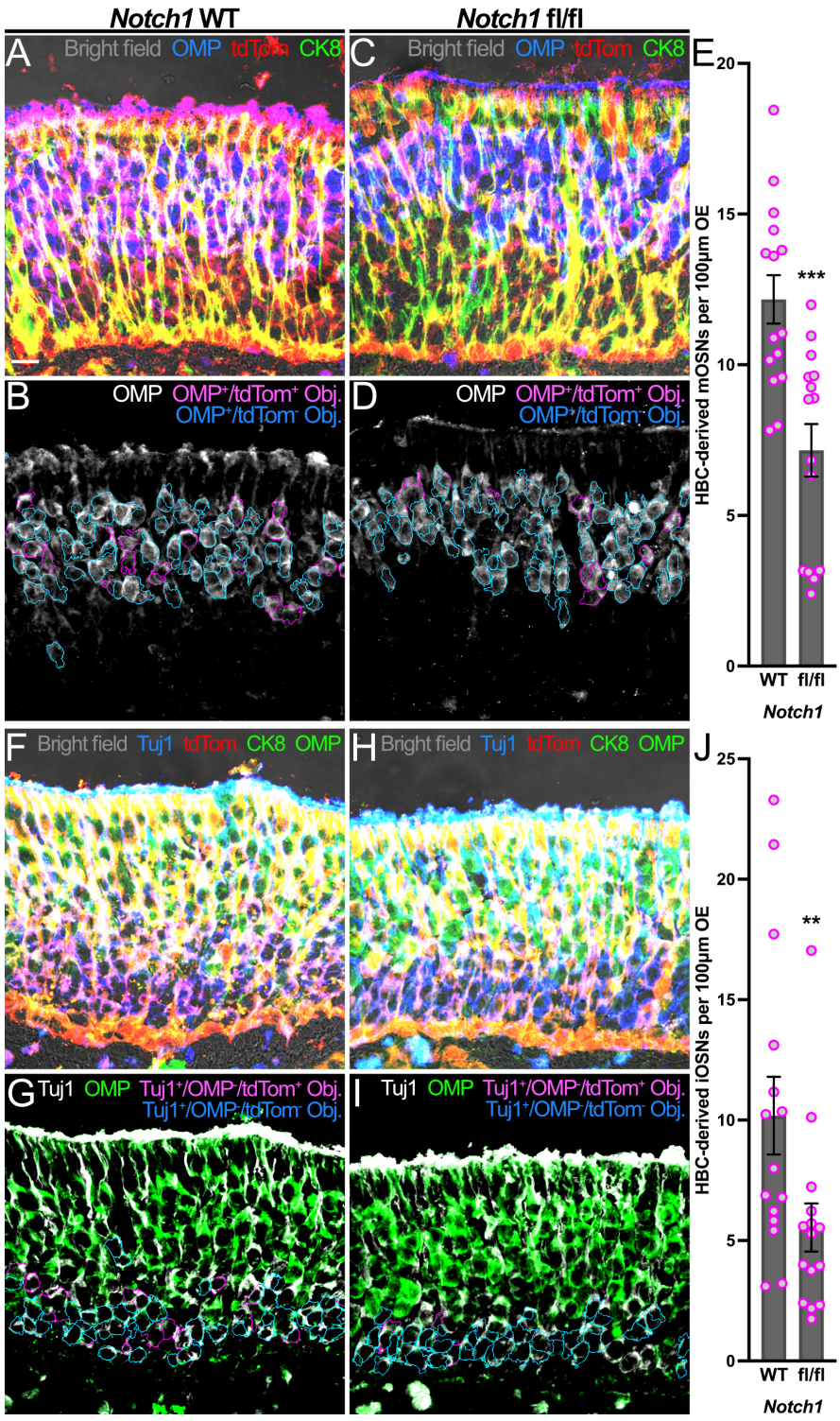

Fig. S6. HBC differentiation into mOSNs and iOSNs following OE injury is attenuated by *Notch1* cKO. A-D: Relative to control (A, B), fewer HBC-derived OMP$^+$/tdTom$^+$ mOSNs (magenta in A and C; magenta outlines in B and D) constitute the morphologically regenerated OE at 28 dpi following HBC-specific *Notch1* cKO (C, D). E: Each circle represents an analyzed region as represented in B and D (n = 3 mice, 15 *Notch1* WT regions and 15 *Notch1* fl/fl regions). F-I: HBC differentiation into Tuj1$^+$/OMP$^-$

/tdTom^{+} iOSNs (magenta in F and H; magenta outlines in G and I) decreases at 28 dpi following following HBC-specific *Notch1* cKO (H, I). J: Each circle represents an analyzed region as represented in G and I (n = 3 mice, 15 *Notch1* WT regions and 15 *Notch1* fl/fl regions). Error bars indicate mean ± s.e.m., Mann-Whitney test, **p<0.01, ***p<0.001 (E, J). Scale bar equals 10 μm (A).

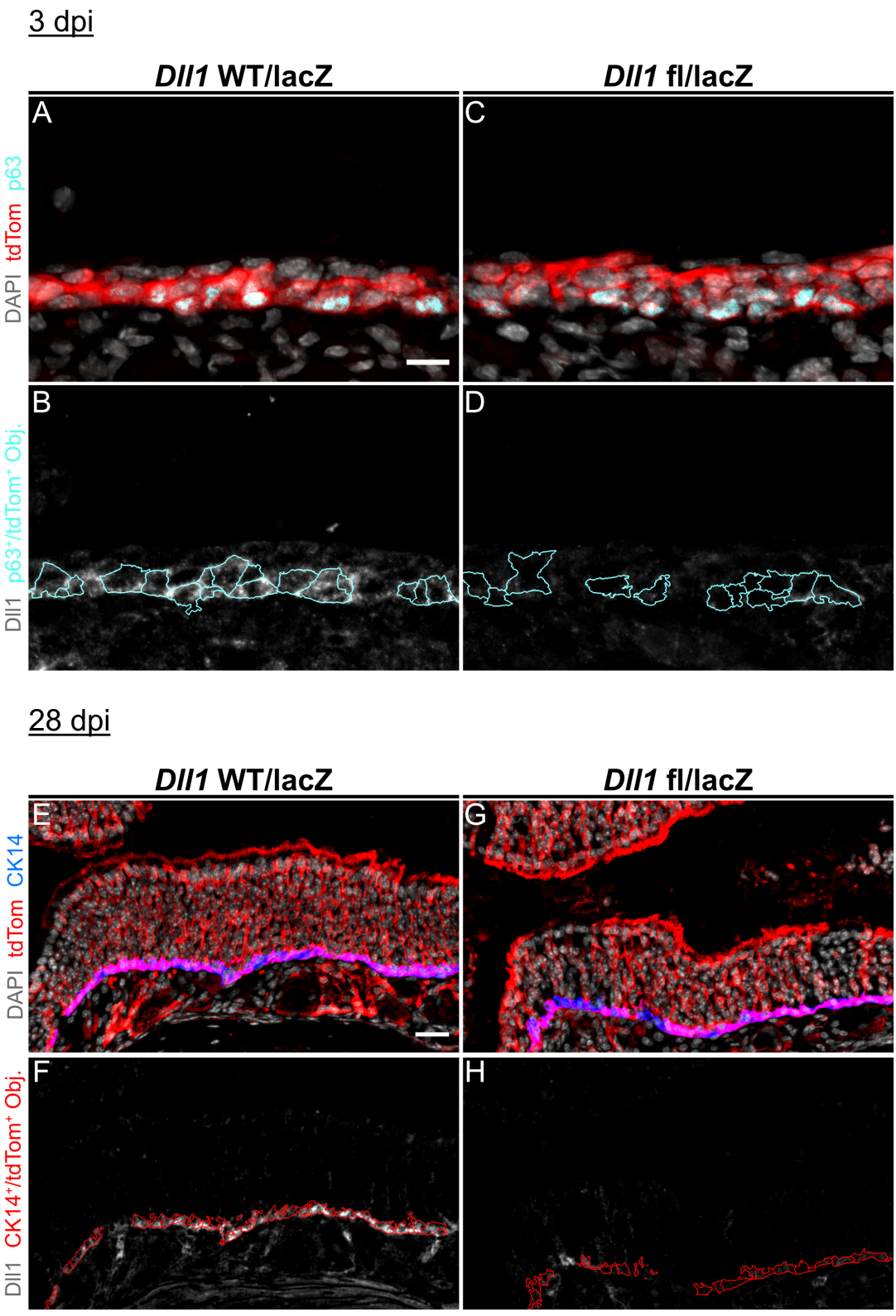

Fig. S7. *Dll1* cKO at various stages of OE regeneration. Images representing the effect of tamoxifen-induced recombination on *Dll1* expression within tdTom$^+$ HBCs (cyan outlines in B and D; red outlines in F and H) at 3 dpi (A-D) and 28 dpi (E-H). Scale bar equals 10 μm (A) and 25 μm (E).

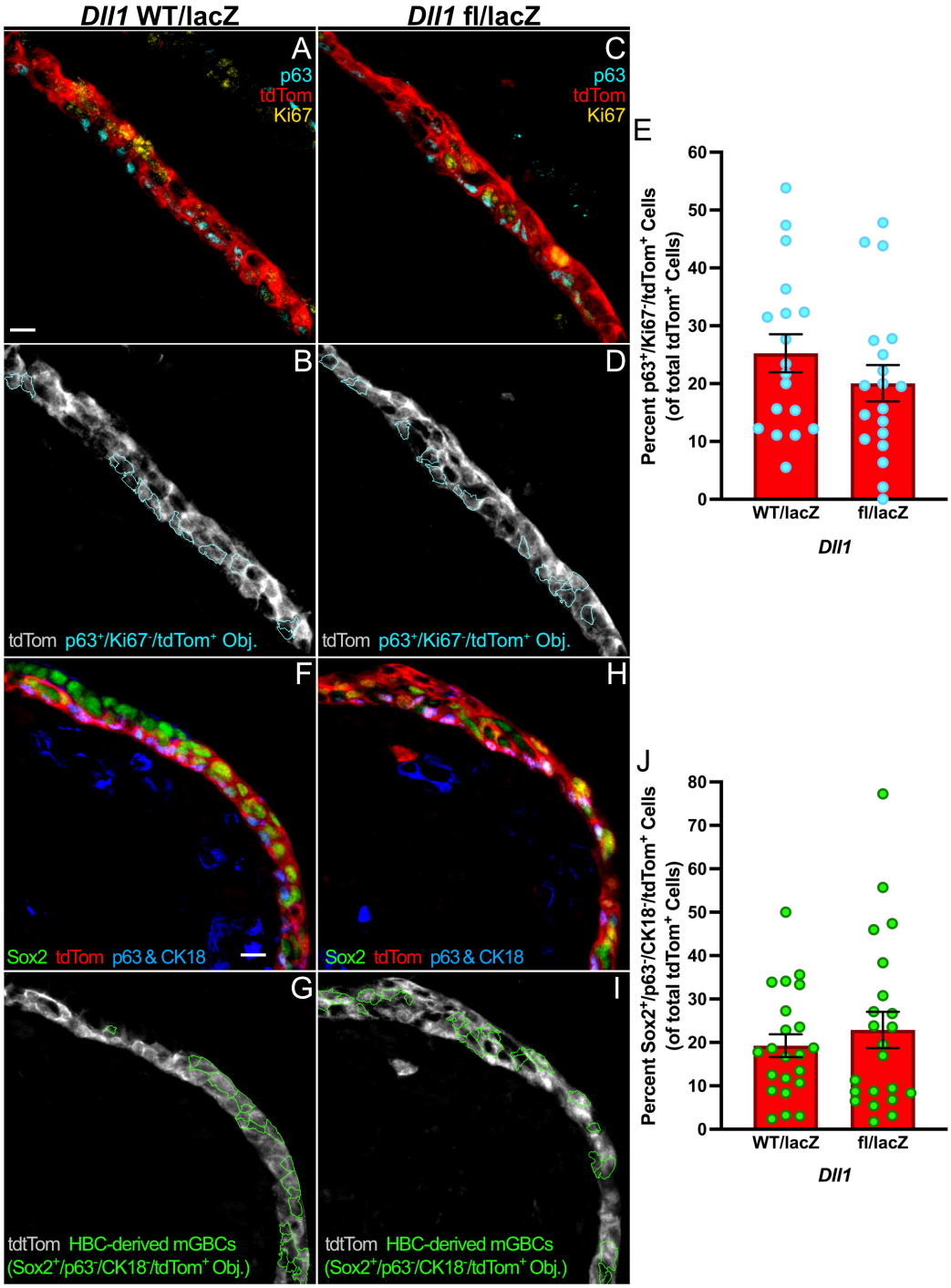

Fig. S8. HBC quiescence and differentiation into mGBCs at 3 dpi is not affected by complete *Dll1* KO. A-D: Relative to control (A, B), the percentage of quiescent HBCs (cyan outlines, B and D) within the regenerating OE at 3 dpi does not significantly change following HBC-specific complete *Dll1* KO (C, D). E: Each circle represents an analyzed region as represented in B and D (n = 3 mice, 18 *Dll1* WT/lacZ regions and 19 *Dll1* fl/lacZ regions). F-I: Relative to control (F, G), the percentage of HBCs that differentiate into Sox2$^+$/p63$^-$/CK18$^-$/tdTom$^+$ mGBCs (green outlines, G and I) within the regenerating OE at 3 dpi does not significantly change following HBC-specific complete *Dll1* KO (H, I). J: Each circle

represents an analyzed region as represented in G and I (n = 3 mice, 22 *Dll1* WT/lacZ regions and 22 *Dll1* fl/lacZ regions). Unpaired t-test (E), Mann-Whitney test (J). Error bars indicate mean ± s.e.m. (E, J). Scale bar equals 10 μm (A).

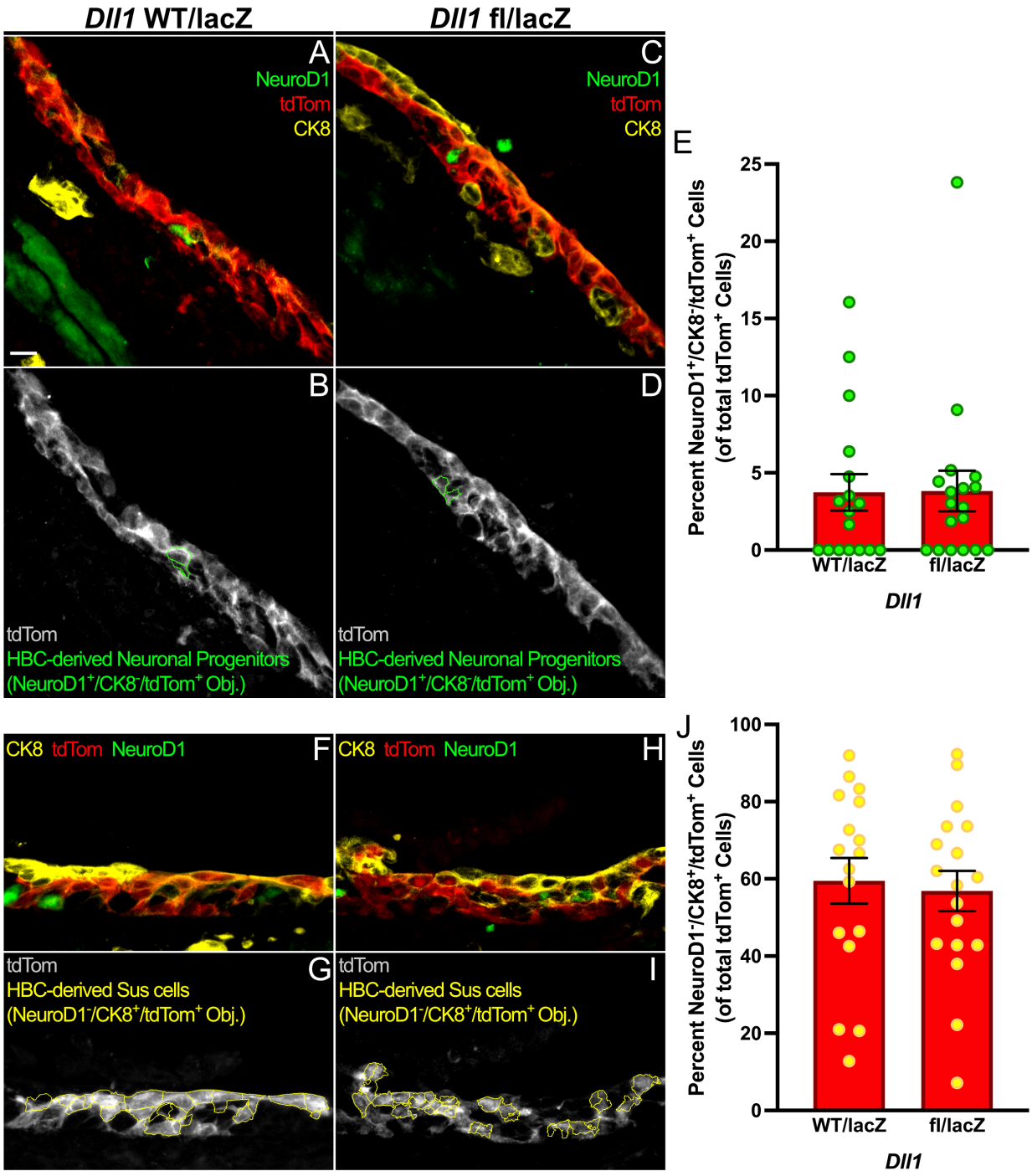

Fig. S9. HBC differentiation into neuronal progenitors and Sus cells at 3 dpi is not affected by complete *Dll1* KO. A-D: Relative to control (A, B), the percentage of HBCs that differentiate into NeuroD1^{+}/CK8^{-}/tdTom^{+} neuronal progenitors (green outlines, B and D) within the regenerating OE at 3 dpi does not significantly change following HBC-specific complete *Dll1* KO (C, D). E: Each circle represents an analyzed region as represented in B and D (n = 3 mice, 17 *Dll1* WT/lacZ regions and 18 *Dll1* fl/lacZ regions). F-I: Relative to control (F, G), the percentage of HBCs that differentiate into

NeuroD1^{-}/CK8^{+}/tdTom^{+} Sus cells (yellow outlines, G and I) within the regenerating OE at 3 dpi does not significantly change following HBC-specific complete *Dll1* KO (H, I). J: Each circle represents an analyzed region as represented in G and I (n = 3 mice, 17 *Dll1* WT/lacZ regions and 18 *Dll1* fl/lacZ regions). Mann-Whitney test (E), unpaired t-test (J). Error bars indicate mean ± s.e.m. (E, J). Scale bar equals 10 μm (A).

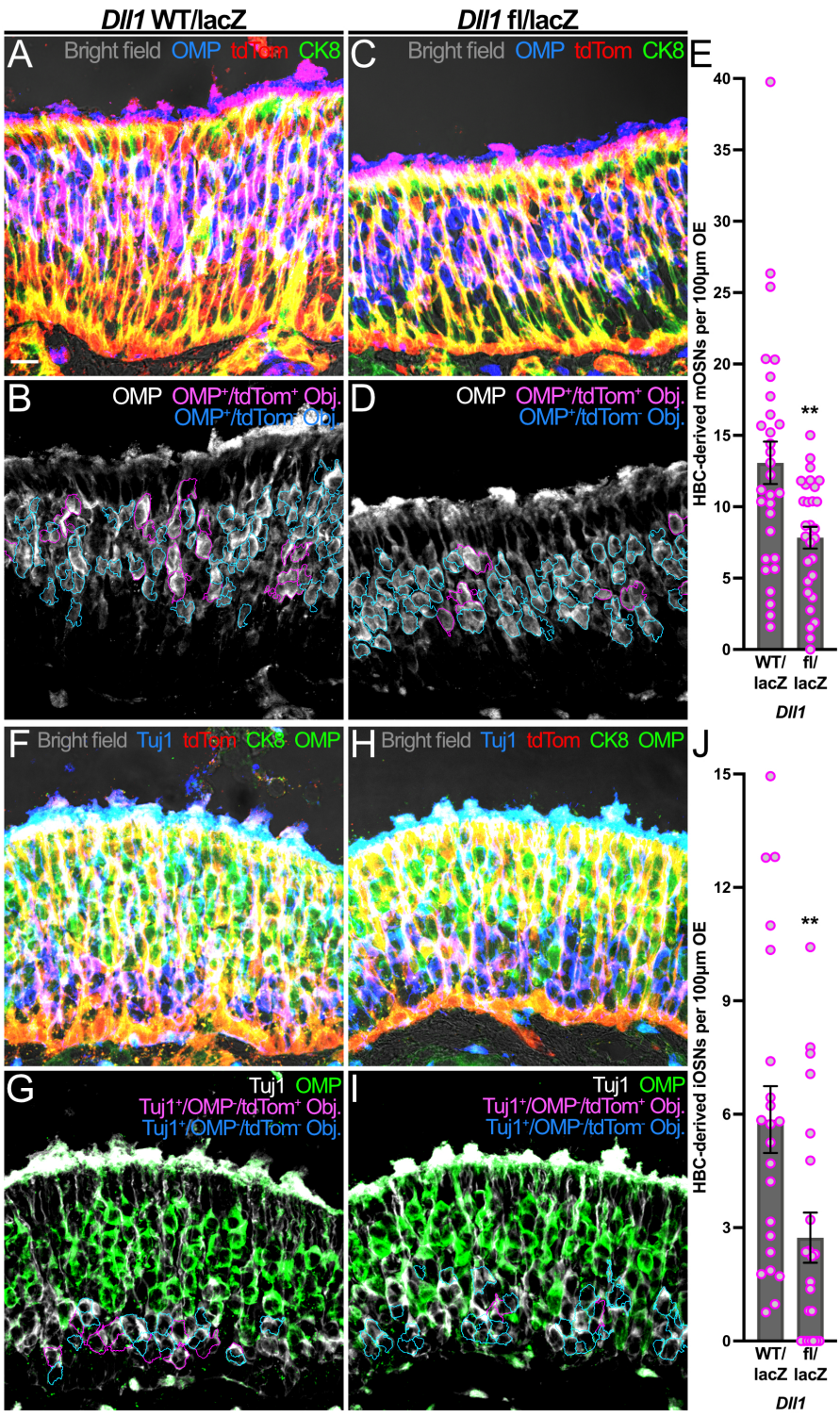

Fig. S10. HBC differentiation into mOSNs and iOSNs following OE injury is attenuated by complete *Dll1* KO. A-D: Relative to control (A, B), HBCs give rise to fewer OMP$^+$/tdTom$^+$ mOSNs (magenta in A and C; magenta outlines in B and D) at 28 dpi following complete *Dll1* KO. E: Each circle represents an analyzed region as represented in B and D (n = 3 mice, 30 *Dll1* WT/lacZ regions and 29 *Dll1* fl/lacZ regions). F-I: Relative to control (F, G), HBC differentiation into Tuj1$^+$/OMP$^-$/tdTom$^+$ iOSNs

(magenta in F and H; magenta outlines in G and I) decreases at 28 dpi following complete *Dll1* KO. J: Each circle represents an analyzed region as represented in G and I (n = 3 mice, 22 *Dll1* WT/lacZ regions and 22 *Dll1* fl/lacZ regions). Error bars indicate mean ± s.e.m., Mann-Whitney test, **p<0.01 (E, J). Scale bar equals 10 μm (A).

Table S1. Antibodies used and associated antigen labeling conditions

Antibody	Source	Identifier	Dilution	Antigen Retrieval	Signal Detection
Mouse α-p63	ATCC	Clone 4A4	1:100	Yes	Secondary fluorophore
Rabbit α-Notch1	Cell Signaling Technology	3608	1:75	Yes	TSA
Rabbit α-Hes1	Cell Signaling Technology	11988	1:50	Yes	TSA
Sheep α-Dll1	R&D Systems	AF3970	1:20	No	TSA
Chicken α-CK5	Biolegend	Clone Poly9059	1:200	No	Secondary fluorophore
Chicken α-mCherry	Novus	NBP2-25158	1:100	No	Secondary fluorophore
Goat α-mCherry	Scigen	AB0040-200	1:50	No	Secondary fluorophore
Rabbit α-Ki67	Abcam	ab15580	1:250	Yes	Secondary fluorophore
Goat α-NeuroD1	R&D Systems	AF2746	1:40	Yes	TSA
Rat α-CK8	Developmental Studies Hybridoma Bank	TROMA-I	1:100	No	Secondary fluorophore
Rabbit α-CK18	Proteintech	10830-1-AP	1:400	No	Secondary fluorophore
Rat α-Sox2	Invitrogen	14-9811-82	1:200	Yes	Secondary fluorophore
Rabbit α-PGP9.5	Proteintech	14730-1-AP	1:200	Yes	Secondary fluorophore
Goat α-IL33	R&D Systems	AF3626	1:10	Yes	Secondary fluorophore
Rabbit α-NICD	Cell Signaling Technology	4147	1:25	Yes	TSA
Mouse α-Tuj1	Biolegend	Clone AA10	1:75	Yes	Secondary fluorophore
Goat α-OMP	Wako Chemicals USA	019-22291	1:100	Yes	Secondary fluorophore